JOURNAL OF AGRICULTURAL AND FOOD CHEMISTRY

Article

pubs.acs.org/JAFC

Binding Patterns and Structure–Affinity Relationships of Food Azo Dyes with Lysozyme: A Multitechnique Approach

Wei Peng,[†,‡,●] Fei Ding,[*,‡,§,●] Yu-Kui Peng,[*,†] Yu-Ting Jiang,[∥] and Li Zhang[⊥]

[†]College of Food Science & Engineering, Northwest A&F University, Yangling 712100, China

[‡]Department of Chemistry, China Agricultural University, Beijing 100193, China

[§]Department of Biological Engineering, Massachusetts Institute of Technology, Cambridge, MA 02139, United States

[∥]Department of Chemistry, University of Ottawa, 10 Marie Curie, Ottawa, ON K1N 6N5, Canada

[⊥]Key Laboratory of Pesticide Chemistry and Application Technology, Ministry of Agriculture, Department of Applied Chemistry, China Agricultural University, Beijing 100193, China

ABSTRACT: Food dyes serve to beguile consumers: they are often used to imitate the presence of healthful, colorful food produce such as fruits and vegetables. But considering the hurtful impact of these chemicals on the human body, it is time to thoroughly uncover the toxicity of these food dyes at the molecular level. In the present contribution, we have examined the molecular reactions of protein lysozyme with model food azo compound Color Index (C.I.) Acid Red 2 and its analogues C.I. Acid Orange 52, Solvent Yellow 2, and the core structure of azobenzene using a combination of biophysical methods at physiological conditions. Fluorescence, circular dichroism (CD), time-resolved fluorescence, UV–vis absorption as well as computer-aided molecular modeling were used to analyze food dye affinity, binding mode, energy transfer, and the effects of food dye complexation on lysozyme stability and conformation. Fluorescence emission spectra indicate complex formation at 10^{-5} M dye concentration, and this corroborates time-resolved fluorescence results showing the diminution in the tryptophan (Trp) fluorescence mainly via a static type (K_{SV} = 1.505 × 10^4 M^{-1}) and Förster energy transfer. Structural analysis displayed the participation of several amino acid residues in food dye protein adducts, with hydrogen bonds, $\pi-\pi$ and cation$-\pi$ interactions, but the conformation of lysozyme was unchanged in the process, as derived from fluorescence emission, far-UV CD, and synchronous fluorescence spectra. The overall affinity of food dye is 10^4 M^{-1} and there exists only one kind of binding domain in protein for food dye. These data are consistent with hydrophobic probe 8-anilino-1-naphthalenesulfonic acid (ANS) displacement, and molecular modeling manifesting the food dye binding patch was near to Trp-62 and Trp-63 residues of lysozyme. On the basis of the computational analyses, we determine that the type of substituent on the azobenzene structure has a powerful influence on the toxicity of food dyes. Results from this work testify that model protein, though an indirect method, provides a more comprehensive profile of the essence of toxicity evaluation of food dyes.

KEYWORDS: *food azo dye, lysozyme, fluorescence, circular dichroism, molecular modeling, structure–affinity relationship*

INTRODUCTION

Based on the Color Index, which is managed by the Society of Dyers and Colorists and American Association of Textile Chemists and Colorists, now more than 10 000 various types of dyes are synthesized and usable in the world; consequently, under these circumstances, one may say that dyes create the world's most gorgeous displays through colored substances.[1] From the available literature, it can be appraised that the total dye utilization worldwide is more than 800 000 tons per year, and among these dyes, azo colorants are the largest and most versatile class of dyes, exceeding 2000 different azo dyes in current use.[2] Azo dyes have a coloring effect involving one or more azo group (−N═N−) in their molecular structure, and they are widely used for coloring textiles, paper, leather, drug, cosmetics, ink, and particularly in food products, due to their variety of color shades, superior fastness, high stability, brilliant colors, and ease of application.[3,4] Because azo dyes are heavily applied and even illegally used in food coloring, coloring in food is an integral part of our culture and is also indispensable to the modern day consumer. They must be present in excessive or relatively high concentrations in food products and eventually denote a severe food security conundrum for humans.[5,6]

Actually, the release of those colored foods and the distribution in the body was photographed and showed that artificial food color could possess serious negative effects upon human behavior, impulse control, attention, ability to focus, learning, thinking, and energy level, and children are particularly susceptible to the effects of food dyes, especially those with attention deficit hyperactivity disorder (ADHD) and attention deficit disorder (ADD).[7,8] Recently, Bateman et al.[9] and McCann et al.[10] achieved a randomized, double-blinded, placebo-controlled, crossover test to examine whether uptake of synthesized food colorant and additives impacted childhood behavior. They offered clear evidence of the deleterious influence of man-made food colors and additives on childrens' actions with data from a total population sample and further

Received: June 25, 2013
Revised: December 1, 2013
Accepted: December 2, 2013
Published: December 2, 2013

affirmed that food additives aggravate hyperactive demeanor in children, even through middle childhood. Obviously, this finding indicates that hurtful effects are not only noticed in children with supreme hyperactivity, but they can also be viewed in the common community and with a wide scope of the graveness of hyperactivity.

Historically, the toxicity of azo compounds used in food processing has been investigated since the early 1960s. Epidemiologic studies have clearly shown that azo dyes may be highly toxic and potentially mutagenic and carcinogenic for humans, and their degradation products such as aromatic amines were also known to be carcinogenic.[11] For example, the azo dye Red No. 2 has been proven to be carcinogenic for rats, and unfortunately, this dye was extensively employed as a food colorant in many regions such as North America and the European Union.[12] Brown et al.[13] found that C.I. Acid Red 2 was shown to be mutagenic, and this discovery was sustained in a study by Chung et al.,[14] in which C.I. Acid Red 2 was mutagenic with metabolic activation. They also noted that C.I. Acid Red 2 is mutagenic when motivated by male Sprague−Dawley rat liver homogenate preparation, and it can be transformed into the mutagenic metabolite *N*,*N*-dimethyl-*p*-phenylenediamine by rat microsomal homogenate azoreductase; it is thereby reasonable that *N*,*N*-dimethyl-*p*-phenylenediamine is the actual mutagen yielded from C.I. Acid Red 2.[15] In another study, C.I. Acid Red 2 was found to be mutagenic just after metabolic stimulation, and the maximum growth in the amounts of revertants for *Salmonella typhimurium* strains TA98, YG1041, and YG1042 strains were 15-fold, 11-fold, and 8-fold, respectively; these outcomes displayed that metabolic variation of C.I. Acid Red 2 resulted in frameshift and substitution mutations, maybe via the begetter of mutagenic nitro derivatives that both the azo chemicals and dross pose in the dyes.[16] Experiments by Sharma et al.[17] explained that C.I. Acid Red 2 possesses a large noxious influence on animal physiology than the healthful effect on the trial organism, and C.I. Acid Red 2 toxicity toward fish was about 2−7-fold under different conditions; LC_{50} data of C.I. Acid Red 2 was 27.2 ppm during acute exposure, and oxygen stress is one of the basic elements in conveying C.I. Acid Red 2 toxicity.

Although azo dyes exhibited generally low acute toxicity, some azo dyes and their metabolites have been confirmed to lead to bladder cancer in humans (e.g., the metabolite of Acid Orange 7, 1-amino-2-naphthol has been reported to induce bladder tumors by Bonser et al.) Acid Red 112, previously utilized as a food dye, was converted through reduction in vitro by *Fusobacterium* sp. 2 into a mutagenic metabolite, which was classified as 2,4,5-trimethylaniline.[19] What's more, some specific cytosolic proteins are involved in the translocation of carcinogenic metabolites of azo dyes from liver cytoplasm into the nucleus. Micronucleus tests have been performed to evaluate the level of the oxidative DNA damage and lipid peroxidation. The results demonstrated that azo dyes (in particular, Sudan Red G) could enhance DNA migration and the micronuclei frequencies at all tested concentrations in a dose-dependent manner, which can influence individual human susceptibility to other environmental carcinogens and have a significant effect on cancer risk.[20]

It is also noteworthy that the azo dyes have numerous structural varieties that are exceedingly stable under exposure to light and resistant to aerobic biodegradation by bacteria. Because of its poisonous properties and that the usage amount of food azo dyes increase daily, the existence of different azo dyes in foodstuffs in our life may represent a harmful risk for human health.[21,22] Therefore, azo compounds have attracted a great deal of attention from many areas of food chemistry and food toxicology. According to the commonly approved concept today, the molecular recognition of food dyes with proteins is able to affect their distribution and biomacromolecule function; on this account, the analysis of their binding to proteins symbolizes an exceptionally important tool to gain toxicological information, particularly ones in the human and animal body.[23,24] Like other biological macromolecules such as polysaccharides and nucleic acids, proteins are essential parts of organisms and participate in virtually every process within cells. Plenty of them are enzymes that catalyze biochemical reactions and are vital to metabolism. Nearly all the small molecules and polypeptides complex with different proteins once they enter the human body. The unique binding property of a protein accounst for the principal role it can play in both the efficacy and the rate of delivery of ligands, usually through the formation of a noncovalent complex, thus influencing the absorption, distribution, metabolism, excretion, and toxicity (ADMET) of diverse substances and affecting the traits of their physiological function.[25] In this work, a low-molecular-weight protein, such as lysozyme, was selected as the model protein, which is a key enzyme and has many physiological and pharmaceutical functions.

Lysozyme was discovered and named by Alexander Fleming in 1922, and it is occasionally called muraminidase or more strictly *N*-acetylmuramide glycanohydrolase.[26] Lysozyme is pervasive in both the animal and plant kingdoms, and, for example, body fluids such as tears, saliva, urine, and human milk contain 2.6, 0.13, trace, and 0.2−0.4 mg mL^{-1} of lysozyme, respectively.[27] As is well-known, the kidney is entailed in the metabolism of diverse endogenous and exogenous ligands, and these chemicals are condensed in the kidney before being excreted by the urine.[28] Within the kidney, different enzymes are included in the biotransformation of varied compounds, and the low-molecular-weight proteins (here lysozyme) are unreservedly percolated in the glomerulus and then reabsorbed through the proximal tubular cells by receptor interfered endocytosis.[29] After endocytosis, an endocytic cyst (endosome) is shaped that is changed to the lysosomes soon after. The ligand−lysozyme complex tracks a similar route as the endogenous lysozyme and finishes up in the lysosomes of the proximal tubular cells. In the lysosome, the compound is thereafter discharged from the macromolecule, either through proteolytic or hydrolytic effects, and is eliminated from the lysosomes into the cytoplasm of the cells.[30] Later, the loosed chemical may operate either within the tubular cell or far downstream after evacuation into the urine or it may recede into the renal venous loop. Lysozyme does not accumulate to an ample degree in tissues elsewhere in the human body except kidney, and the ligand−lysozyme conjugation can be solid within the recursion to restrain precocious systemic effects minus the effects of the free ligand.[31] It is thereby proper to deliberate the function of the low-molecular-weight protein lysozyme in influencing concrete ligand binding, pharmacokinetics, and toxicokinetics.

Given this background, the goal of the current task was to assess the molecular recognition as well as the spatial structure of the complexes formed between lysozyme and the model food azo dyes, C.I. Acid Red 2 (structure shown in Figure 1) by employing steady-state and time-resolved fluorescence, circular dichroism, hydrophobic probe ANS (8-anilino-1-naphthalene-

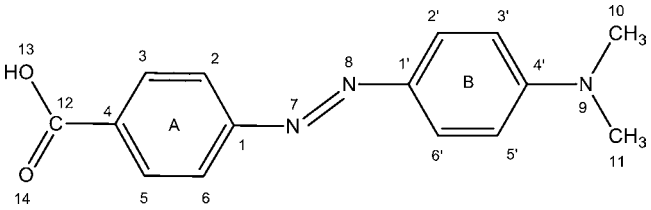

Figure 1. Molecular structure of C.I. Acid Red 2.

sulfonic acid), and UV−vis absorption along with computer-aided molecular modeling. Specifically, we also chose two frequently used food azo dyes (C.I. Acid Orange 52 and Solvent Yellow 2) that are structurally similar to C.I. Acid Red 2 and their core functional group azobenzene for the specialized analysis of the general binding mode between lysozyme and food azo dyes by computational docking. This study tries to unveil the feature recognition and the changes in the conformation of the protein as well as attempts to understand the toxicological information of food azo dyes.

EXPERIMENTAL SECTION

Material. Lysozyme from chicken egg white (L4919, BioUltra, lyophilized powder, ≥98%) and C.I. Acid Red 2 (32 654, CAS Number: 493-52-7) used in this study were purchased from Sigma-Aldrich (St. Louis, MO) and used without further purification, and deionized water was produced by a Milli-Q Ultrapure Water Purification System from Millipore (Billerica, MA). All of the experiments were performed in Tris (0.2 M)-HCl (0.1 M) butter of pH = 7.4, with an ionic strength of 0.1 in the presence of NaCl, and the pH was checked with an Orion Star A211 pH Benchtop Meter (Thermo Scientific, Waltham, MA). Dilutions of the lysozyme stock solution (10 μM) in Tris-HCl butter were prepared immediately before use, and the concentration of lysozyme was determined by the method of Lowry et al.[32] All other reagents employed were of analytical grade and received from Sigma-Aldrich.

Steady-State Fluorescence. Steady-state fluorescence was conducted with a 1.0 cm path length quartz cell using a F-7000 spectrofluorimeter (Hitachi, Japan) equipped with a thermostatic bath and a microcomputer. The excitation and emission slits were set at 5.0 nm each, intrinsic fluorescence was obtained by exciting the continuously stirred lysozyme solution at 295 nm to selectively excite the Trp residues, and the fluorescence emission spectra were recorded in the wavelength range of 300−450 nm at a scanning speed of 240 nm min^{-1}. The reference sample consisting of the Tris-HCl buffer and C.I. Acid Red 2 did not give any fluorescence signal.

Circular Dichroism. Far-UV CD spectra were recorded with a Jasco-815 spectropolarimeter (Jasco, Japan) equipped with a microcomputer, and the instrument was calibrated with d-10-camphorsulfonic acid. All the CD spectra were carried out at 298K with a PFD-425S Peltier temperature controller attached to a water bath with an accuracy of ±0.1 °C. Each spectrum was registered with use of a quartz cell of 1.0 cm path length and taken at wavelengths between 200 and 260 nm with 0.1 nm step resolution and averaged over five scans recorded at a speed of 20 nm min^{-1} and a response time of 1 s. All observed CD spectra were baseline subtracted for buffer, and the secondary structure was computed exploiting Jasco Spectra Manager II, which calculates the different designations of secondary structures by comparison with CD spectra, determined from distinct proteins for which high-quality X-ray diffraction data are available.[33]

Time-Resolved Fluorescence. Time-resolved fluorescence was acquired with a FLS920 spectrometer (Edinburgh Instruments, UK), using the time-correlated single-photon counting system with a hydrogen flash lamp excitation source, in air equilibrated solution at an ambient temperature. The excitation wavelength was 295 nm and the number of counts gathered in the channel of maximum intensity was 4000. The instrument response function (IRF) was conducted exploiting Ludox to scatter light at the excitation wavelength. The data were analyzed with a nonlinear least-squares iterative method utilizing the Fluorescence Analysis Software Technology, which is a sophisticated software package designed by Edinburgh Photonics for the analysis of fluorescence and phosphorescence decay kinetics. The IRF was deconvoluted from the experimental data, and the resolution limit after deconvolution was 0.2 ns. The value of χ^2 (0.9−1.2), the Durbin−Watson parameter (greater than 1.7), as well as a visual inspection of the residuals were used to assess how well the calculated decay fit the data. Average fluorescence lifetime (τ) for multi-exponential function fittings were from the following relation:[34]

$$I(t) = \sum_i A_i e^{-t/\tau_i} \quad (1)$$

where τ_i are fluorescence lifetimes and A_i are their relative amplitudes, with i variable from 1 to 2.

ANS Displacement. In the first series of experiments, lysozyme concentration was kept fixed at 1.0 μM, C.I. Acid Red 2/ANS concentration was varied from 10 to 70 μM, and lysozyme fluorescence was recorded (λ_{ex} = 295 nm, λ_{em} = 340 nm). In the second series of experiments, C.I. Acid Red 2 was added to solutions of lysozyme and ANS held in equimolar concentration (1.0 μM), C.I. Acid Red 2 concentration was also varied from 10 to 70 μM, and the fluorescence of ANS was collected (λ_{ex} = 370 nm, λ_{em} = 465 nm).

Molecular Modeling. Molecular modeling of the lysozyme−food azo dyes complexation was carried out on an SGI Fuel Workstation. The crystal structure of lysozyme (PDB code: 6LYZ), determined at a resolution 2.0 Å, was retrieved from the Brookhaven Protein Data Bank (http://www.rcsb.org/pdb) as a docking template. After importation into the program Sybyl version 7.3 (http://tripos.com), the protein structure was strictly checked for atom and bond type correctness assignment. Hydrogen atoms were computationally added using the Sybyl 7.3 Biopolymer and Build/Edit menus. To avoid negative acid/acid interactions and repulsive steric clashes, added hydrogen atoms were energy minimized with the Powell algorithm with a convergence gradient of 0.5 kcal (mol Å)$^{-1}$ for 1500 cycles; this procedure does not change positions of heavy atoms, and the potential of the three-dimensional structure of lysozyme was assigned according to the AMBER force field with Kollman all-atom charges. The two-dimensional structures of C.I. Acid Red 2, C.I. Acid Orange 52, Solvent Yellow 2, and azobenzene was downloaded from PubChem (http://pubchem.ncbi.nlm.nih.gov), and the initial structure of the molecules was generated by Sybyl 7.3. The geometry of these four azo compounds was subsequently optimized to minimal energy using the Tripos force field with MMFF94 charges; the Surflex-Dock program, which employs an automatic flexible docking algorithm, was applied to calculate the possible conformation of the ligand that binds to the protein, and the program PyMOL (http://www.pymol.org)

was finally used for visualization of the molecular docking results.

Principle of Fluorescence Quenching. Fluorescence quenching refers to any process that decreases the fluorescence intensity of a sample. A variety of molecular interactions can result in quenching, such as excited state reactions, molecular rearrangements, energy transfer, ground state complex formation, and collisional quenching. Fluorescence quenching is described by the well-known Stern−Volmer equation:[34]

$$\frac{F_0}{F} = 1 + k_q\tau_0[Q] = 1 + K_{SV}[Q] \quad (2)$$

In this equation, F_0 and F are the fluorescence intensities in the absence and presence of quencher, respectively, k_q is the bimolecular quenching constant, τ_0 is the lifetime of the fluorophore in the absence of quencher, $[Q]$ is the concentration of quencher, and K_{sv} by linear regression of a plot of F_0/F versus $[Q]$.

Calculation of Affinity Constant. When ligand molecules bind independently to a set of equivalent sites on a macromolecule, the equilibrium between free and bound ligand molecules is given by the following relation:[35]

$$\log\frac{F_0 - F}{F} = n\log K - n\log\frac{1}{[Q_t] - \frac{F_0 - F}{F_0}[P_t]} \quad (3)$$

where F_0 and F are the fluorescence intensities in the absence and presence of quencher, respectively, K and n are the association constant and the number of binding sites, respectively, and $[Q_t]$ and $[P_t]$ are the total concentration of quencher and protein.

Statistical Analysis. All assays were executed in triplicate, and the mean values, standard deviations, and statistical differences were estimated using analysis of variance (ANOVA). The mean values were compared using a Student's *t*-test, and all statistic data were treated using the OriginPro Software (OriginLab Corporation, Northampton, MA).

RESULTS

Fluorescence of the Lysozyme−C.I. Acid Red 2 Complex. Basically, binding of a ligand to a protein may alter the ground and excited state properties of both the protein and the ligand, and accordingly, variation of different spectroscopic characteristics (e.g., fluorescence intensity, shapes, lifetime, etc.) is extensively certified for the ligand's probing polarity or hydrophobicity, shaping aggregation deranged upon protein conjugation, selectively binding in one of their protonation states, or experiencing protein transfer reactions.[36] Figure 2 shows the raw fluorescence data of lysozyme at pH = 7.4 with different amounts of C.I. Acid Red 2 following an excitation at 295 nm. Lysozyme displayed a strong fluorescence emission peak at 340 nm, and the addition of C.I. Acid Red 2 created an evident shrink of the fluorescence signal. Fluorescence intensity was gradually narrowed by increasing the concentration of C.I. Acid Red 2, and under the experimental conditions, C.I. Acid Red 2 displayed no fluorescence emission in the range of 300−450 nm, which did not affect lysozyme. The quenching of the intrinsic Trp fluorescence obviously explained the complex of C.I. Acid Red 2 with lysozyme, as C.I. Acid Red 2 is located in the region where Trp is situated within or near the fluorophore. Furthermore, the maximum emission wavelength shifted from 339.6 to 340.4 nm, but we do not think that the bathochromic

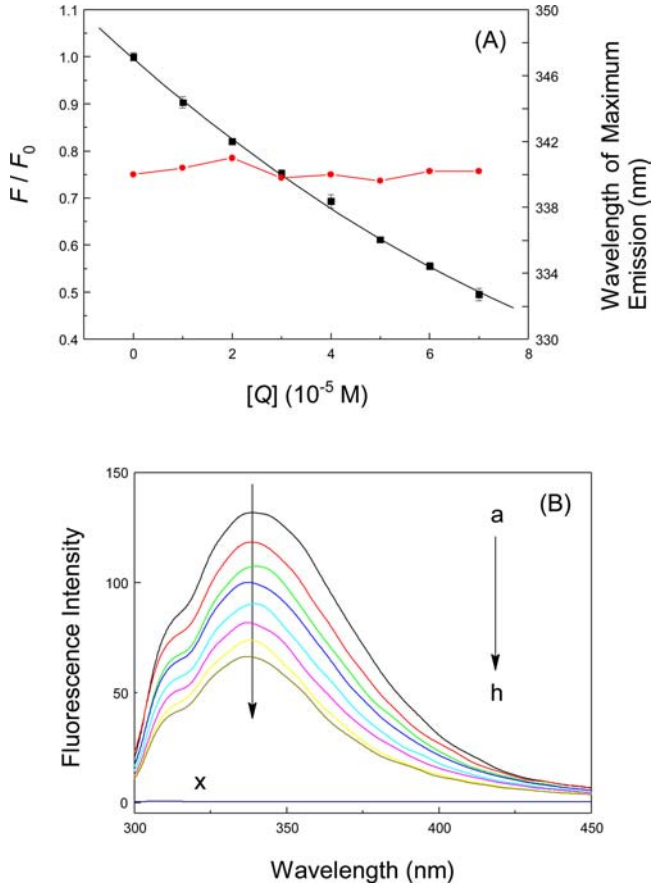

Figure 2. (A). Tryptophan fluorescence quenching of lysozyme at pH = 7.4 and T = 298 K, plotted as extinction of lysozyme tryptophan (F/F_0) against C.I. Acid Red 2 concentration. The fluorescence emission intensity was recorded at λ_{ex} = 295 nm, and the λ_{em} maximum occurred at 340 nm. All data were corrected for quencher fluorescence, and each data point was the mean of three independent determinations ± SD ranging from 0.62 to 1.44%. (B) Shows fluorescence emission spectra of lysozyme (1.0 μM) in the presence of different concentrations of C.I. Acid Red 2, (a)→(h): c(C.I. Acid Red 2) = 0, 10, 20, 30, 40, 50, 60, and 70 μM; (x) 70 μM C.I. Acid Red 2 only.

shift can be regarded as evidence to prove conformational changes of lysozyme.

In order to confirm this corollary, circular dichroism was applied to quantitatively analyze the secondary structural changes of lysozyme. Generally, the characterization of CD spectra is a powerful analytical method to study the association of proteins with other ligands and to determine the protein conformation in solution;[37] therefore, the far-UV CD spectra of lysozyme in the absence and presence of C.I. Acid Red 2 were scanned in Figure 3, and secondary structure components computed based on raw CD data are collected in Table 1. The CD curves of lysozyme displayed two negative peaks in the far-UV CD region at 208 and 222 nm, characteristic of an α-helical structure of lysozyme.[33] Free lysozyme has 44.7% α-helix, 18.3% β-sheet, 13.9% turn, and 23.1% random coil. After complexing with C.I. Acid Red 2, a decrease in α-helix was seen from 44.7% (free lysozyme) to 43.8% (complex), while there was an increase in β-sheet, turn, and random coil from 18.3, 13.9, and 23.1% free lysozyme to 18.5, 14.3, and 23.4% (complex) at a molar ratio of lysozyme to C.I. Acid Red 2 of 1:80. However, the changes of secondary structure are not

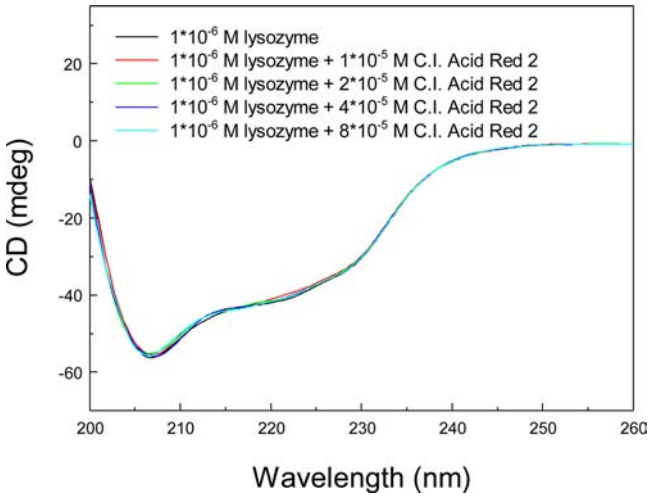

Figure 3. Far-UV CD spectra of the lysozyme−C.I. Acid Red 2 mixture (pH = 7.4, T = 298 K). (a) 1.0 μM lysozyme in the presence of 0 (black), 10 (red), 20 (green), 40 (blue), and 80 (cyan) μM C.I. Acid Red 2.

Table 1. Secondary Structure of Lysozyme Complexes with C.I. Acid Red 2 at pH = 7.4 Calculated by Jasco Spectra Manager II

	secondary structure components (%)			
c(dye) (μM)	α-helix	β-sheet	turn	random
0	44.7	18.3	13.9	23.1
10	43.1	18.8	14.6	23.5
20	42.8	18.8	14.1	24.3
40	44.1	18.4	14.2	23.3
80	43.8	18.5	14.3	23.4

enough to give rise to destabilize the lysozyme spatial structure. Furthermore, the structural changes examined by far-UV CD spectra are in good agreement with steady-state fluorescence and also conform with the synchronous fluorescence below.

Synchronous fluorescence was introduced by Lloyd in 1971, and it can offer the information about the molecular environment in the vicinity of the chromophore molecules.[38] According to the theory of Miller, when the D-value ($\Delta\lambda$) between excitation and emission wavelengths was fixed at 15 or 60 nm, the synchronous fluorescence gives the distinctive information of Tyr or Trp residues.[39] The effect of C.I. Acid Red 2 on lysozyme synchronous fluorescence is shown in Figure 4; a slight red shift can be observed (from 280 to 281 nm) when $\Delta\lambda$ = 60 nm, and had no shift when $\Delta\lambda$ = 15 nm, but the bathochromic effect shall be rested in experimental error. The fluorescence intensity diminished regularly with the addition of C.I. Acid Red 2, which further demonstrated the occurrence of fluorescence quenching in the association.

Binding Property. To interpret the data from steady-state fluorescence quenching, it is important to apprehend what kind of interaction happens between the C.I. Acid Red 2 and the lysozyme. Thereby the quenching data were analyzed according to the Stern−Volmer equation (eq 2), and the corresponding results fitted from Stern−Volmer plots Figure 5 were summarized in Table 2. The results visibly evidence that the Stern−Volmer quenching constant, K_{sv}, is the opposite correlated with temperature, and the value of k_q is 100-fold higher than the maximum value for diffusion-controlled quenching in water (~10^{10} M^{-1} s^{-1}), indicating that the

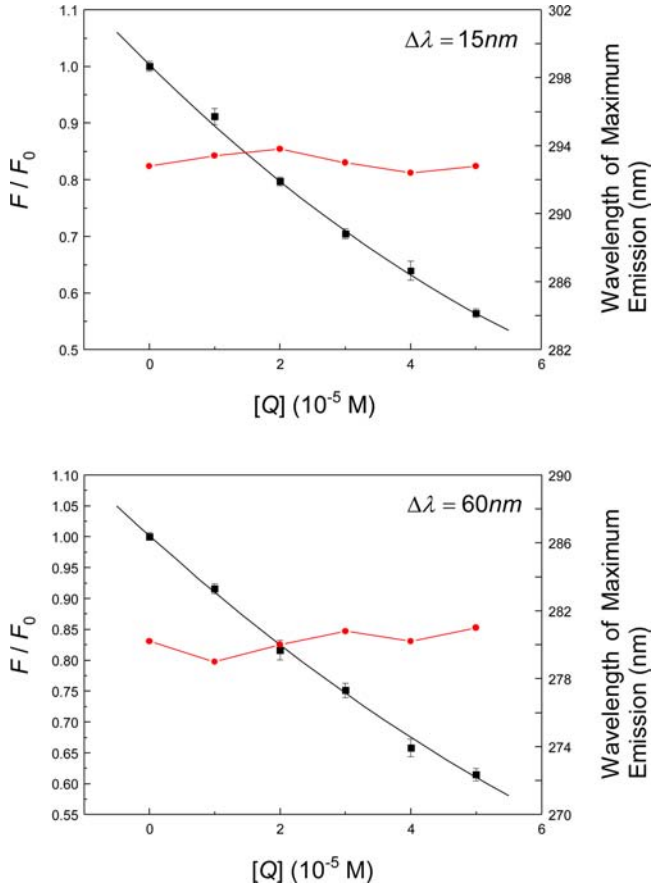

Figure 4. Relationships between synchronous fluorescence intensity ($\Delta\lambda$ = 15 nm and $\Delta\lambda$ = 60 nm) and maximum emission wavelength of lysozyme at pH = 7.4 and T = 298 K, plotted as extinction of lysozyme tryptophan (F/F_0) versus C.I. Acid Red 2 concentration. Each point was the average of three individual experiments ± SD ranging from 0.62% to 1.62%.

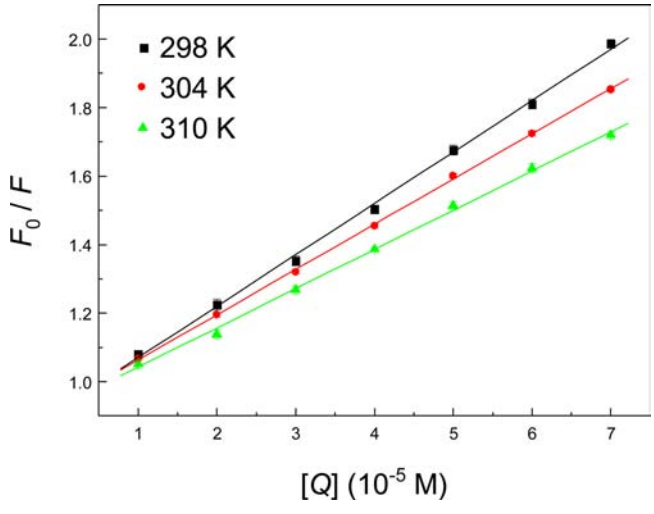

Figure 5. Stern−Volmer plots describing fluorescence quenching of lysozyme in the presence of different concentrations of C.I. Acid Red 2. Each data point was the mean of three separate observations ± SD ranging from 0.59 to 1.62%.

probable quenching mechanism for lysozyme fluorescence by C.I. Acid Red 2 is a static type[40] because higher temperature

dx.doi.org/10.1021/jf4039327 | J. Agric. Food Chem. 2013, 61, 12415−12428

Table 2. Stern–Volmer Quenching Constants, Affinities, and Thermodynamic Parameters for the Association of Lysozyme with C.I. Acid Red 2 at Different Temperatures[a]

T (K)	K_{SV} ($\times 10^4$ M^{-1})	k_q ($\times 10^{12}$ M^{-1} s^{-1})	R^a	K ($\times 10^4$ M^{-1})	n	R^a	$\Delta H°$ (kJ mol^{-1})	$\Delta G°$ (kJ mol^{-1})	$\Delta S°$ (J mol^{-1} K^{-1})
298	1.505 ± 0.01253	7.798 ± 0.01253	0.9992	1.039 ± 0.01715	1.06	0.9998	−45.33	−22.91	−75.29
304	1.321 ± 0.01149	6.845 ± 0.01149	0.9998	0.7047 ± 0.00965	1.05	0.9991		−22.39	
310	1.149 ± 0.01388	5.953 ± 0.01388	0.9989	0.5119 ± 0.02005	1.02	0.9976		−22.01	

[a] R is the correlation coefficient.

will typically result in the dissociation of weakly bound complexes and, as a result, smaller amounts of static quenching.

The dissimilar accessibilities of Trp residues in proteins have resulted in the customary application of quenching to settle the approachable and unreachable residues. In the presence of quencher, the strength of the reachable fraction (f_a) is reduced according to the Stern–Volmer equation, whereas the concealed fraction is not quenched. Therefore, the relationship between the modified Stern–Volmer quenching constant and the accessible fraction is given by[41]

$$\frac{F_0}{\Delta F} = \frac{F_0}{F_0 - F} = \frac{1}{K_a f_a [Q]} + \frac{1}{f_a} \quad (4)$$

where F_0 and F are the fluorescence intensities in the absence and presence of quencher, respectively, f_a is the fraction of the initial fluorescence that is accessible to quencher, K_a is the modified Stern–Volmer quenching constant of the accessible fraction, and $[Q]$ is the concentration of quencher. This modified figure of the Stern–Volmer allows K_a to be determined graphically (Figure 6), and the result was found

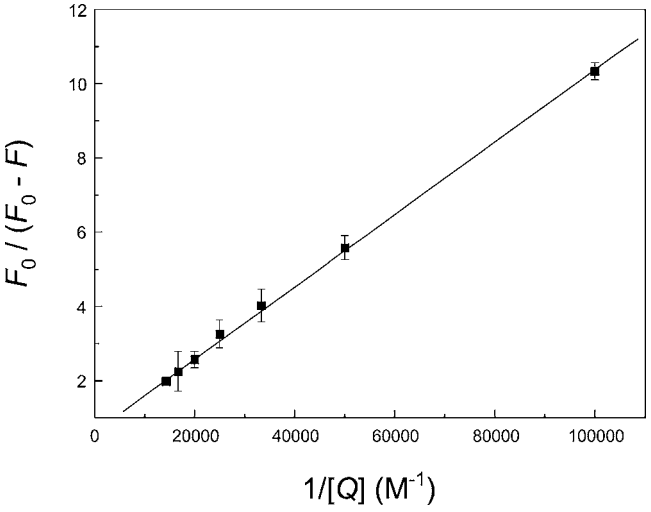

Figure 6. Modified Stern–Volmer plot displaying tryptophan quenching of lysozyme (1.0 μM) at pH = 7.4 and T = 298 K in the presence of different concentrations of C.I. Acid Red 2. Fluorescence emission intensity was recorded at λ_{ex} = 295 nm, and the λ_{em} maximum occurred at 340 nm.

to be $K_a = 7.212 \times 10^3$ M^{-1} (R = 0.9995), implying intelligibly that the efficient association constant for the ligand–biopolymer mixture pertains to moderate intensity;[42] this data coincides with our binding affinity and the location discussion based on eq 3, ANS experiments, and molecular docking simulations.

Essentially, static and dynamic quenching can be distinguished through their differing dependence on temperature, but fluorescence quenching is best studied by time-resolved fluorescence measurements, which can discriminated between static and dynamic processes directly.[34] Thus, representative fluorescence decay pictures of lysozyme at various molar ratios of C.I. Acid Red 2 in Tris-HCl buffer, pH = 7.4 are shown in Figure 7, and the fluorescence lifetime and their amplitudes are

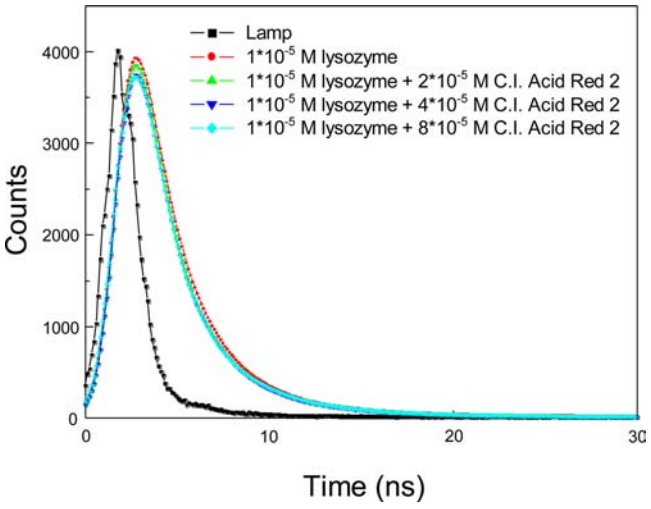

Figure 7. Time-resolved fluorescence decays of lysozyme in Tris-HCl buffer, pH = 7.4, c(lysozyme) = 10 μM; c(C.I. Acid Red 2) = 0 (red), 20 (green), 40 (blue), and 80 (cyan) μM. The sharp pattern on the left (black) is the lamp profile.

Table 3. Fluorescence Lifetime of Lysozyme as a Function of the Concentrations of C.I. Acid Red 2

samples	τ_1 (ns)	τ_2 (ns)	A_1	A_2	τ (ns)	χ^2
free lysozyme	1.33	3.15	0.67	0.33	1.93	1.08
lysozyme + C.I. Acid Red 2 (1: 2)	1.28	3.26	0.76	0.24	1.76	1.02
lysozyme + C.I. Acid Red 2 (1: 4)	1.25	3.16	0.79	0.21	1.65	1.05
lysozyme + C.I. Acid Red 2 (1: 8)	1.32	3.21	0.85	0.15	1.60	1.09

also collected in Table 3. The decay curves fitted well to a biexponentical function with an emerging relative fluorescence lifetime of τ_1 = 1.33 ns and τ_2 = 3.15 ns of lysozyme, while in the maximum concentration of C.I. Acid Red 2, the lifetime is τ_1 = 1.32 ns and τ_2 = 3.21 ns. As Trp is known to divulge multiexponential decays, a clear allocation of the perceived separate fluorescence lifetime components to the disparate fluorescent Trp residues is diffult to determine for multiple Trp residues proteins such as lysozyme. Thus, we have not tried to designate the independent components; conversely, the average fluorescence lifetime has been utilized in order to proceed with a qualitative analysis. The average lifetime of lysozyme did not

change evidently, only from 1.93 to 1.60 ns, at different C.I. Acid Red 2 concentrations, stating patently that fluorescence quenching is essentially static mechanism.[43,44] Moreover, the fluorescence lifetime of one ingredient (τ_1) is nearly equal for all the four systems, but the fluorescence lifetime of another constituent (τ_2) expanded upon complexation of C.I. Acid Red 2, which explains lucidly that a lysozyme-food dye complex is generated between the fluorophore and C.I. Acid Red 2 and that this complex is nonfluorescent.

Thermodynamic Analysis. The molecular recognition of an edge in the action of ligand−acceptor interactions, especially when the acceptor is an enzyme or a drug receptor, has ignited the interest of a group of investigators with a realistic motivation to understand the structure and function of artificial and biological complexes for the design of new ligands such as pharmaceuticals, pesticides, or other biological agents. Because the essence of most ligand−acceptor recognition includes reasonably infirm noncovalent interactions that result from electrostatic attractions, hydrogen bonds, van der Waals, or hydrophobic interactions, they are classically promptly mutable and thereby amenable to standard equilibrium thermodynamic analysis.[45] The thermodynamic parameters dependent on temperatures were analyzed to describe the acting forces between lysozyme and C.I. Acid Red 2, and the signs and magnitudes of thermodynamic parameters for protein recognition can account for the primary forces contributing to protein stability. Usually, if the enthalpy change ΔH° does not vary prominently over the temperature range studied, then its data can be measured from the van't Hoff equation:

$$\ln K = \frac{-\Delta H^\circ}{RT} + \frac{\Delta S^\circ}{R} \quad (5)$$

$$\Delta G^\circ = \Delta H^\circ - T\Delta S^\circ \quad (6)$$

where K is the binding affinity for a given association reaction under a specified set of experimental conditions, R is the gas constant, T is the absolute temperature, and the superscript "°" shows the value of the property of a molar concentration of unity. From the linear relationship between ln K and $1/T$ (Figure 8), the thermodynamic parameters were received and listed in Table 2. The negative sign for ΔG° means that the molecular recognition process was spontaneous, and the formation of the macromolecule−ligand complex was an exothermic reaction accompanied by a negative ΔS° value. Ross and Subramanian[46] have summarized the signs and magnitudes of the thermodynamic parameters associated with various individual types of interaction that may happen in protein association processes, as described below. For typical hydrophobic effect, both ΔH° and ΔS° are positive, while they are negative for van der Waals forces and hydrogen bond formation in low dielectric medium. Further, specific electrostatic interactions between ionic species in aqueous solution were expressed by a positive value of ΔS° and a negative ΔH° (almost zero). A negative ΔH° value is observed whenever there are hydrogen bonds in the binding events. In the present case of the lysozyme−C.I. Acid Red 2 complex, the negative ΔH° (−45.33 kJ mol^{-1}) and ΔS° (−75.29 J mol^{-1} K^{-1}) attested that both hydrogen bonds and van der Waals forces play a foremost role in the molecular recognition of food dye by biomacromolecule.

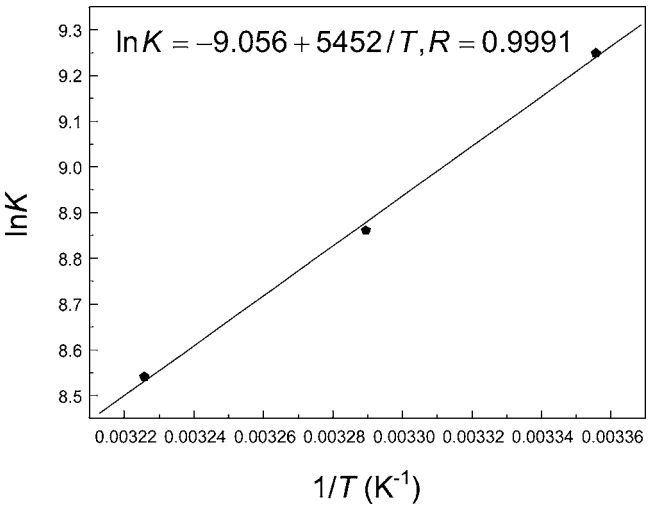

Figure 8. van't Hoff plot for the molecular recognition of C.I. Acid Red 2 by lysozyme in Tris-HCl buffer, pH = 7.4.

Binding Affinity and Location. It is well-known that the physiological function of a protein is decided by its structure. Binding of ligands to proteins normally evokes a change to their three-dimensional structures, resulting in an alteration of absorption. Hence, the form of ligand is regarded as pharmacologically or toxicologically active, and its function associates mainly with the protein−ligand affinity.[47] To calculate the affinity of food dye to lysozyme, eq 3 was used to calculate K and n by linear regression of a plot of the $\log((F_0 - F)/F$ versus $\log(1/([Q_t]-(F_0-F)[P_t]/F_0))$, and the results were found to be $K = 1.039 \times 10^4$ M^{-1} and $n = 1.06$ (298 K). According to Kragh−Hansen,[48] the affinity computed for the lysozyme-food azo dye implied a moderate binding with respect to the other strong protein−ligand complexes with affinities ranging from 10^6 to 10^8 M^{-1}. The experimental data ΔG° is highly approaching the theoretical value $\Delta G^\circ = -23.74$ kJ mol^{-1}, demonstrating the dependability of the outcomes of steady-state fluorescence analysis. Additionally, the value of n is approximately equal to 1, which may bear out the existence of just one kind of binding site in lysozyme for C.I. Acid Red 2.[49] The intrinsic fluorescence of lysozyme is primarily owning to the Trp-62, from the value of n. The C.I. Acid Red 2 binding site is most likely adjacent to this residue, which engenders fluorescence quenching.[50]

Fluorescence dye ANS, 8-anilino-1-naphthalenesulfonic acid, is known to bind hydrophobic domains of proteins and can play the role of a sensitive reporter of conjugation in the neighborhood of protein Trp residues; thus, it has been used to describe all the hydrophobic sites of proteins.[51] To further depict the quiddity of the complex between lysozyme and C.I. Acid Red 2, binding assays were achieved in the presence of ANS under the same conditions, and the relative fluorescence intensity (F/F_0) against ligand concentration ([Ligand]) plot is listed in Figure 9. At a ligand concentration of 70 μM, both C.I. Acid Red 2 and ANS decrease Trp residue fluorescence, but the level of quenching by ANS was less than that of C.I. Acid Red 2—ANS could quench about 39%, while C.I. Acid Red 2 could curtail approximately 50% of Trp fluorescence. When C.I. Acid Red 2 is added to the ANS−lysozyme system, it can compete with ANS and displace ANS from its binding site, and the fluorescence would decrease because ANS is essentially nonfluorescent when in aqueous solution. However, it will become highly fluorescent in nonpolar solvents or when it is bound to protein.[52] As can be seen from Figure 9, in the presence of C.I. Acid Red 2, the ANS−lysozyme system

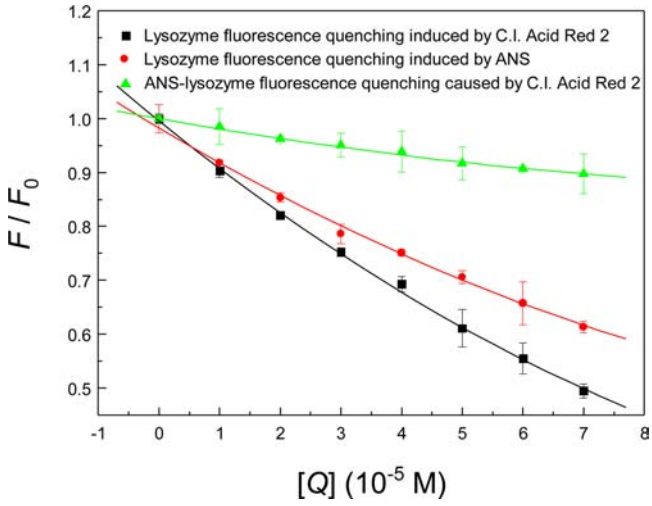

Figure 9. Fluorescence quenching isotherm of lysozyme induced by different concentrations of C.I. Acid Red 2 (■) and ANS (●), respectively, and c(C.I. Acid Red 2) = c(ANS) = 0, 10, 20, 30, 40, 50, 60, and 70 μM; and fluorescence quenching profile of ANS-lysozyme caused by various amounts of C.I. Acid Red 2 (▲), c(C.I. Acid Red 2) = 0, 10, 20, 30, 40, 50, 60, and 70 μM; pH = 7.4, T = 298 K. Each point was the average of three individual measurements ± SD ranging from 0.33% to 3.95%.

fluorescence compressed about 10%, which corroborates the following molecular modeling simulations laying the C.I. Acid Red 2 at the hydrophobic domain, and attesting that hydrogen bonds and $\pi-\pi$ interactions operated between C.I. Acid Red 2 and lysozyme.

Molecular Modeling. Lysozyme is one of the earliest well-characterized and most studied globular proteins due to its tertiary structure that has been solved through X-ray crystallography by Blake et al.[53] According to X-ray diffraction measurement of lysozyme, it is a single, nonglycosylated polypeptide chain of 129 amino acid residues folded in two domains, which contain some water molecules. Both domains are functional for the active site cleft which is formed between them and stabilized by four disulfide bonds. Lysozyme includes six Trp residues at positions 28, 62, 63, 108, 111, and 123, two of which (Trp-62 and Trp-63) are responsible for most of its intrinsic fluorescence. The others in the proximity of the Trp are associated with the sulfur atoms of the disulfide bonds.[54] To further substantiate the interaction between lysozyme and the model food dye, C.I. Acid Red 2, molecular modeling has been selected to realize the nature of the lysozyme−food dye complex, and the best docking energy results are presented in Figure 10. As can be seen from Figure 10, the oxygen atom (O-14) of the carbonyl group and the nitrogen atom (N-8) of azo group in the azo dye can form significant hydrogen bonds with the hydrogen atom of the imino group in Trp-63 and the hydrogen atom of the H_2O-221. The bond lengths, respectively, are 1.9, 2.4, and 2.34 Å. The perpendicular molecular distance between the kernel of the benzene ring and the indole ring in Trp-62 residue and the core of the benzene ring B and azo group in dye is 3.43 and 3.33 Å, which illustrated the existence of evident $\pi-\pi$ and cation$-\pi$ interactions between the lysozyme and the food dye molecule. As mentioned previously, the crystal structure of lysozyme involves some water molecules, and these water molecules have great influence on the association process via bridge linkage. For example, the hydroxyl group in azo dye could interact with Asn-59 and Ala-107 residues in lysozyme through H_2O-206 and H_2O-198. The distance between hydroxyl group in azo dye and Asn-59 and Ala-107 residues in lysozyme and H_2O-206 and H_2O-198 is 2.05, 2.03, 2.09, and 3.18 Å, respectively. Therefore, we can not disregard this feature because water bridge linkage interactions act as an important role in nature, especially in protein structure and molecular recognition.

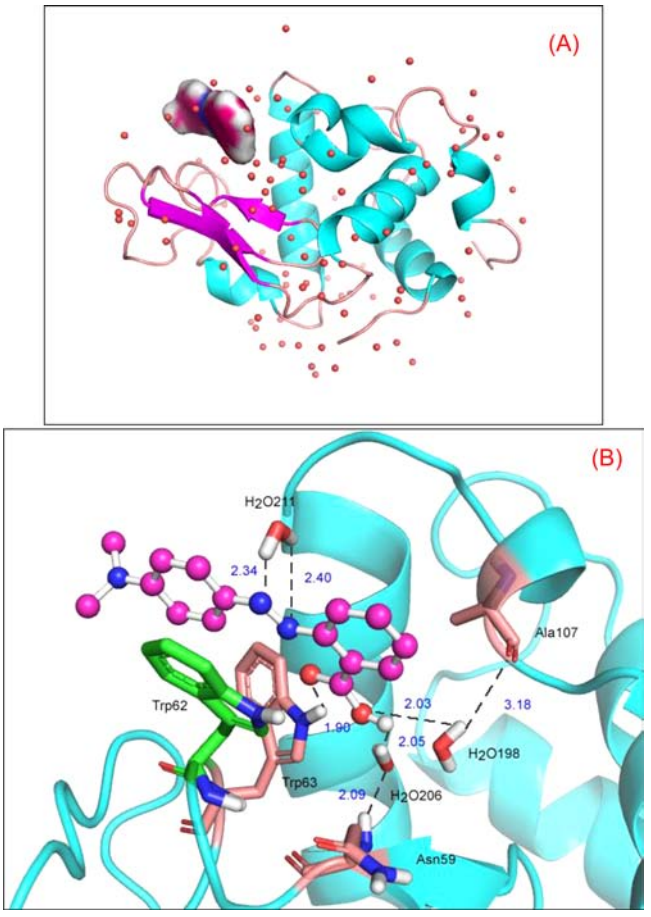

Figure 10. Molecular modeling of C.I. Acid Red 2 docked to lysozyme. Panel (A) shows docked C.I. Acid Red 2 into the lysozyme at the active site; lysozyme represented in surface colored in cyan, to C.I. Acid Red 2, colored as per the atoms and possess translucent surface of electron spin density. Panel (B) displays the amino acid residues involved in binding of C.I. Acid Red 2; the ball-and-stick model indicates C.I. Acid Red 2, colored as per the atoms and the key amino acid residues around C.I. Acid Red 2 has been depicted with the stick model; the pink stick model reveals hydrogen bonds between Trp-63 and H_2O-221 and C.I. Acid Red 2; the green stick model explains $\pi-\pi$ and cation$-\pi$ interactions between Trp-62 and C.I. Acid Red 2. (For interpretation of the references to color in this figure legend, the reader is referred to the web version of the article.).

Energy Transfer. Förster resonance energy transfer (FRET) has been broadly employed in all practical applications of fluorescence due to the advantageous distance for energy transfer, which are characteristically the size of a protein or the thickness of a membrane. FRET arises between a donor molecule in the excited state and an acceptor molecule in the ground state. The donor normally emits at shorter wavelengths that overlap with the absorption spectrum of the acceptor, and FRET befalls without the advent of a photon and is the consequence of long-range dipole−dipole interactions between the donor and acceptor.[55,56] Here, the spectral overlap between

the fluorescence emission spectrum of lysozyme (donor) and the UV−vis absorption spectrum of C.I. Acid Red 2 (acceptor) is displayed in Figure 11. According to the Förster theory, the

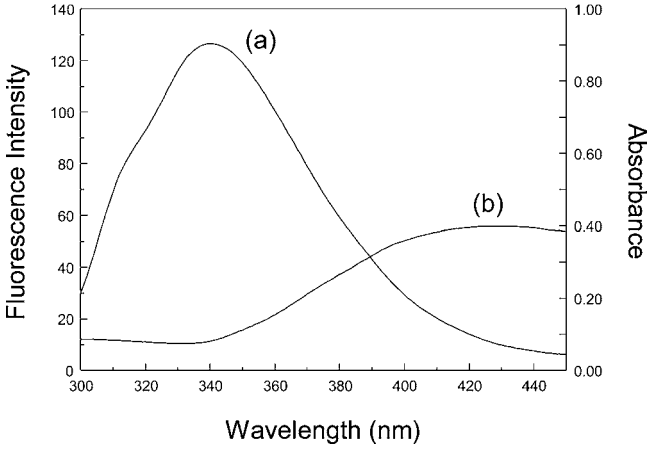

Figure 11. Overlapping between the fluorescence emission spectrum of lysozyme (a) and UV−vis absorption spectrum of C.I. Acid Red 2 (b). c(lysozyme) = 1.0 μM, c(C.I. Acid Red 2) = 70 μM; pH = 7.4, T = 298 K.

rate of energy transfer depends upon the following factors: (*i*) the extent of spectral overlap of the fluorescence emission spectrum of the donor with the UV−vis absorption spectrum of the acceptor, (*ii*) the quantum yield of the donor, (*iii*) the relative orientation of the donor and acceptor transition dipoles, and (*iv*) the distance between the donor and acceptor molecules.[55−57] The efficiency of energy transfer (E) is the fraction of photons absorbed by the donor which are transferred to the acceptor, and this fraction is described by

$$E = \frac{R_0^6}{R_0^6 + r^6} \tag{7}$$

where R_0^6 is the Förster distance, r is the donor-to-acceptor distance, and the Förster distance is given by

$$R_0^6 = 8.79 \times 10^{-25} \times k^2 \times n^{-4} \times \varphi \times J \tag{8}$$

In this equation, k^2 is a factor describing the relative orientation in space of the transition dipoles of the donor and acceptor. k^2 is normally assumed to be equal to 2/3, which is the value for donors and acceptors that randomize by rational diffusion prior to energy transfer. n is the refractive index of the medium, φ is the quantum yield of the donor in the absence acceptor, and the overlap integral J exhibits the degree of spectral overlap between the donor emission and the acceptor absorption:

$$J = \frac{\sum F(\lambda)\varepsilon(\lambda)\lambda^4\Delta\lambda}{\sum F(\lambda)\Delta\lambda} \tag{9}$$

where $F(\lambda)$ is the corrected fluorescence intensity of the donor in the wavelength range λ to $\lambda+\Delta\lambda$ with the total intensity normalized to unity, $\varepsilon(\lambda)$ is the extinction coefficient of the acceptor at λ, which is regularly in units of M^{-1} cm^{-1}. In aqueous media, k^2 = 2/3, n = 1.336, φ = 0.14 for lysozyme;[42] using these parameters, we acquire the following data: J = 1.058 × 10^{14} M^{-1} cm^3, R_0 = 2.55 nm, r = 3.13 nm. The donor-to-acceptor distance lies within the range of 0.5 R_0 < r < 2R_0, revelatory of an effective energy transfer from lysozyme to C.I. Acid Red 2, and further demonstrating that fluorescence quenching was more likely engendered by the static type in addition to nonradiative energy transfer.

DISCUSSION

It appears that the utilization of artificial food coloring is largely the economic matter of rendering foods more charming to the consumer. As mentioned earlier, azo dyes are used throughout in the food processing industries, and they are found virtually exclusively in all the colored foodstuffs such as cake, cream, curd, jam, jelly, packet soup, sauce, soft drink, sweet, wine, and so forth.[58] Although the acceptable daily intake is low, the individual response variation depends not only on dose, age, gender, nutritional status, and genetic factors but also on long-term exposure to low doses. Certain azo dyes are some of the first organic compounds to be associated with human cancer, but very little attention was paid to the safety of coloring materials for food. The possible mechanism of molecular toxicology between the long-term intake of food dyes and various human diseases remains unresolved.[59−61]

All the experiments stated herein indicate that the interaction between lysozyme and C.I. Acid Red 2 occurred smoothly, but the native conformation of lysozyme undergo no changes upon dye conjugation. This phenomenon has been verified by far-UV CD spectra—the strong signal at 208 and 222 nm represents the presence of a heavy proportion of α-helix in lysozyme, which is able to tie food dye. Further, the negative bands between 208 and 209 nm and 222 and 223 nm could probably originate from the contribution by the $n\rightarrow\pi^*$ transition for the peptide bond of the α-helix.[33,37] To put it in another way, the major conformation of lysozyme is also α-helix, and the reduction of α-helix with a growth in the β-sheet, turn, and random coil indicates that C.I. Acid Red 2 bound with amino acid residues of the polypeptide chain.[62,63] This also clearly corroborates fluorescence emission and synchronous fluorescence measurements, which demonstrates that the complexation of C.I. Acid Red 2 with lysozyme does not initiate spatial structure changes in the protein molecule and may be correlated to its physiological activity. It was apparent to all that the bioavailability of a ligand to a target tissue is affected by its binding affinity to protein, and the reversible protein−ligand adduct plays the primary role of a reservoir making free ligand usable when the concentration of the unbound ligand decreases. The unbound concentration of the ligand, thereby the biological activity, hinges on the quantity of ligand bound to protein.[64,65] Steady-state fluorescence, time-resolved fluorescence as well as site-specific ligand ANS explain that the C.I. Acid Red 2 binding site is near Trp-62 and Trp-63 with a moderate affinity of 10^4 M^{-1}. Similar findings have also been depicted by Bourassa et al.[66] and Kanakis et al.[67] for the binding of resveratrol, genistein, and curcumin to milk α- and β-caseins and β-lactoglobulin. Although the affinity between protein and food azo dye does not belong to a strong association, the normal level of protein is high enough to permit enormous conjugation in all probability. As noted above, the strength of complexation with a protein could have momentous importance for the speed of clearance of azo dye and for their transport to cells and tissues. If the unbound dye departs the circulatory system and penetrates tissues or experiences excretion, the disassociation of the protein−food dye coordination must operate promptly to keep the balance between the free and complexed dye concentrations. Therefore, we should pay more attention to this aspect, owing to the fact that protein usually serve as a vector for almost all endogenous

and exogenous ligands in the human body to ship the food dye to the target tissues, where it elicits its toxicological action.

As set forth, protein binding could efficaciously elongate the in vivo half-life of azo dye, even though the concentration of food dye is not very high in many food products. It is more important that these food dyes commonly influence the function of liver and kidney, finally bringing down the enzyme quickly, which is in logical consonance with the comet assay in eight mouse (male ddY mice) organs.[68] Moreover, Amin et al.[69] fulfilled an animal experiments in order to assess the toxic effect of food azo dyes C.I. Acid Yellow 23 and C.I. Acid Red 14 on renal, hepatic function, lipid profile, blood glucose, body-weight gain, and biomarkers of oxidative stress in young male (*Rattus norvegicus*) albino rats. The data realistically signified that a plain increase in alanine transaminase, aspartate transaminase, alkaline phosphatase, urea, creatinine total protein, and albumin in serum of rats dosed with C.I. Acid Yellow 23 and C.I. Acid Red 14 compared to control rats, and therefore, azo dyes can adversely affect and change biochemical markers in vital organs (e.g., liver and kidney, not only at higher doses but also at low doses.

Because of the experimental results and the combination of different evaluations on animal models, we might consider that food azo dye could easily bind to model protein and then reduce protein activity and possibly induce damage of protein, all of these resulting in pathological changes to certain organs such as field cancerization and deformation.[70,71] It is generally known that almost all diseases are thought to be associated with different types of amino acids, thereby Asn-59, Trp-62, Trp-63, and Ala-107 residues and some water molecules (e.g., H_2O-198 and H_2O-206) were found to be critical to the model of the protein−azo dye reaction with the help of computer-aided molecular modeling, and the driving forces in the present case are hydrogen bonds, $\pi-\pi$ and cation$-\pi$ interactions, and water bridge linkage interactions.[72] Chemically, azo compound is characterized by the presence of the chromophoric azo group, but modification of the substitute group on the left or right aromatic ring may have the potential to affect the affinity between the lysozyme and azo dye. In order to confirm this speculation, two other azo dyes, C.I. Acid Orange 52 and Solvent Yellow 2, which has an analogous configuration with C.I. Acid Red 2, and the core azobenzene structure have been chosen for conducting molecular modeling simulations. The best docking energy results are given in Figure 12 and the binding energy, hydrogen bonds, and water bridge linkage interactions are collected in Table 4. Evidently, the binding energy between C.I. Acid Orange 52 and lysozyme is akin to C.I. Acid Red 2. One rationale was that the sulfonic group in C.I. Acid Orange 52 can make hydrogen bonds and bridge linkages with Trp-63 residue, H_2O-198, and H_2O-206; this mode could make the conformation of C.I. Acid Orange 52 more stable at the active site in lysozyme. But for the Solvent Yellow 2, there is just one electron-donating group of less polarity ($-N(CH_3)_2$) in the dye molecule, and this group has the ability to roll over to the Trp-63, H_2O-198, and H_2O-206 nearby. It can then form a hydrogen bond with imino group in Trp-63, and thus the affinity of lysozyme with Solvent Yellow 2 is weaker than that of C.I. Acid Red 2 and C.I. Acid Orange 52. Although hydrogen bonds and $\pi-\pi$ and cation$-\pi$ interactions may be achieved by the core azobenzene structure and H_2O-221 and Trp-62, unluckily, no polar substitutes are located in the molecule, and azobenzene cannot generate strong interactions such as hydrogen bonds with amino acids in

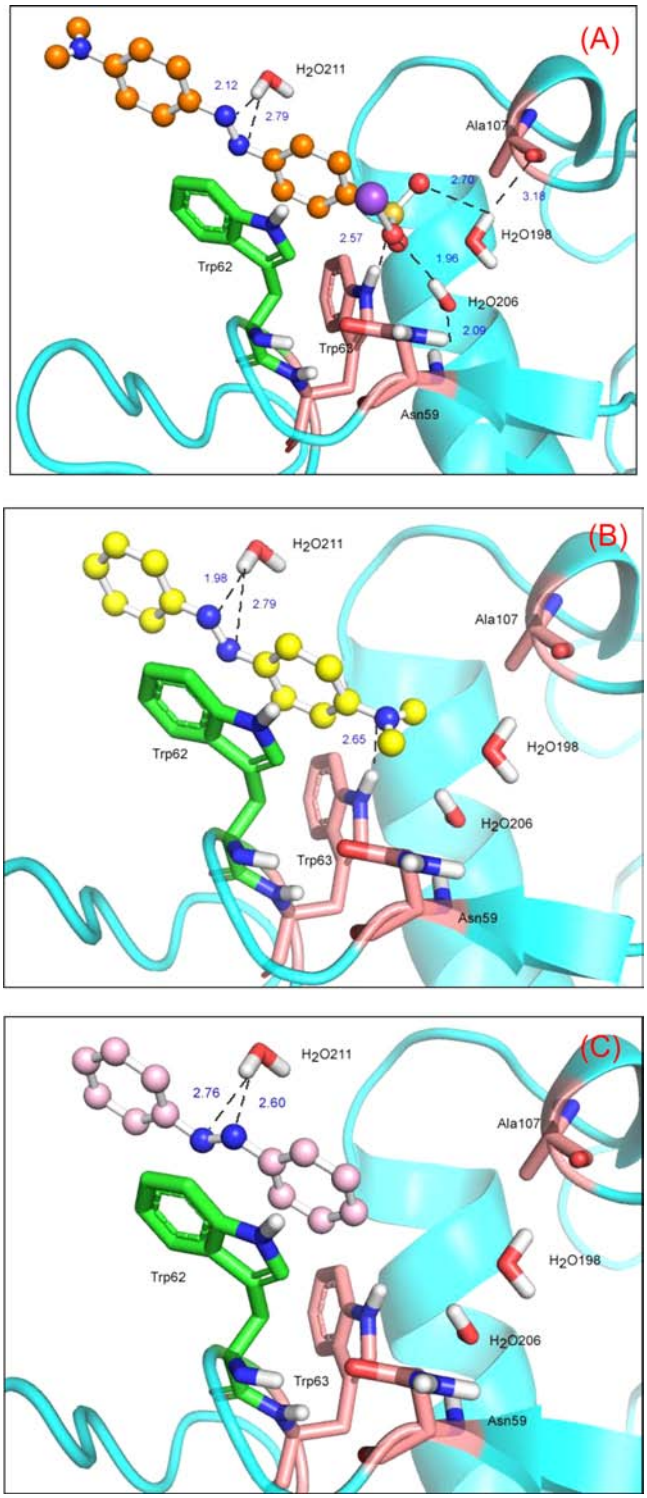

Figure 12. Molecular modeling of C.I. Acid Orange 52 (A), Solvent Yellow 2 (B), and azobenzene (C) docked to lysozyme. Panels (A), (B), and (C) show the amino acid residues involved in binding of (A), (B), and (C). The ball-and-stick model indicates (A), (B), and (C), colored as per the atoms and key amino acid residues around (A), (B), and (C). The pink stick model reveals hydrogen bonds between Trp-63 and (A), (B), and (C). The green stick model explains $\pi-\pi$ and cation$-\pi$ interactions between Trp-62 and (A), (B), and (C). (For interpretation of the references to color in this figure legend, the reader is referred to the web version of the article.).

Table 4. Hydrogen Bonds Analyses from the Results of Molecular Docking for Lysozyme with C.I. Acid Orange 52, Solvent Yellow 2, and Azobenzene

Compounds	Molecular structure	Donor	Acceptor	Distance (Å)
C.I. Acid Orange 52	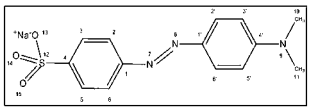	H_2O-221 H	Ligand N-7	2.79
		H_2O-221 H	Ligand N-8	2.12
		Trp-63 NH	Ligand O-13	2.57
		H_2O-206 H	Ligand O-13	1.96
		H_2O-198 H	Ligand O-14	2.70
Solvent Yellow 2	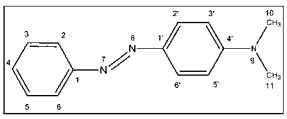	H_2O-221 H	Ligand N-7	2.79
		H_2O-221 H	Ligand N-8	1.98
		Trp-63 NH	Ligand N-9	2.65
Azobenzene	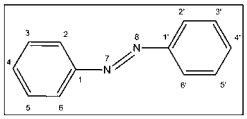	H_2O-221 H	Ligand N-7	2.60
		H_2O-221 H	Ligand N-8	2.76

lysozyme. Therefore, the affinity between azobenzene and lysozyme is the lowest.

By all accounts, the polarity of the substitutes in azobenzene affects the affinity between model azo dye and lysozyme directly, thereby affecting its toxicity. If an electron-withdrawing group is introducted in the benzene ring, the binding capacity of azo dye for lysozyme could be strengthened significantly. Some studies propose that azo dyes are capable of producing cytochrome P450 decrease in animals,[73−75] and the cytochrome P450 decline is magnified by azo dyes, which is substituted by electron-withdrawing groups, compared with those substituted by electron-donating groups. These phenomena may illustrate that the property of a substituent plays a fundamental role in the azo dye−lysozyme association process. As has been argued, a food azo dye with a relatively high protein binding affinity will have a long half-life, which may increase its toxicity. Conversely, an azo dye with a low protein binding affinity is limited in its ability to suffuse tissues and reach the site of action, and such a situation would produce unfavorable effects on the biological activities of proteins.[76,77] Taking all the above information into consideration, whether the food azo dyes substituted by an electron-withdrawing group (e.g., −COOH, $-COOCH_3$, $-AsO_3H_2$, $-SO_3H$) or an electron-donating group (e.g., $-NH_2$, −OH, $-CH_3$) will have a great negative impact on the human body.

What is also vitally important to point out is that the azo compound is a azobenzene derivative composed of two benzene rings linked by a −N═N− double bond, and food azo dye hence could easily be metabolized into an aromatic amine or reduced to substituted naphthol compounds by gut flora, which may also be regarded as the genotoxic agents.[21,78,79] The aromatic amine might further oxidize into nitrosamines and yield reactive oxygen species (ROS) in the process as well. With the increase of ROS, the antioxidant defense enzymes will be consumed for the purpose of preventing the oxidation in cells and induce a drastic reduction of antioxidants in vivo, and the ROS will ultimately lead to carcinosis and mutagenesis in different organs. These results are clearly endorsed by Stingley et al.[80] who have denoted that at least a portion of the human skin microbiota is capable of azo dye (C.I. Acid Red 2 and C.I. Acid Orange 7) reduction and the formation of carcinogenic aromatic amines that are more readily absorbed by the skin than the original dyes.

Overall, the current study elaborates an integrated experimental approach: steady-state fluorescence, far-UV CD, synchronous fluorescence and time-resolved fluorescence, UV−vis absorption, and computer-aided molecular modeling of the complexation of the vastly applied model food azo dye which can be used to color foods such as aperitif drinks and fish roe with the lysozyme, which is also known as muramidase or *N*-acetylmuramide glycanhydrolase under physiological conditions. According to steady-state analysis, the quenching of lysozyme originated from a static mechanism, and this phenomenon coincides with the results based on time-resolved fluorescence measurements that the food dye−protein ground state complex formation occurs with a moderate affinity of 10^4 M^{-1}. Although food dye could interact with the polypeptide chains of lysozyme, the spatial structure of model protein remained unvaried; this result was fully vindicated by far-UV CD and synchronous fluorescence spectra. Through ANS displacement and molecular modeling, we can validate the food dye binding cavity is near the Trp-62 and Trp-63 residues on lysozyme, and hydrogen bonds, $\pi-\pi$ and cation$-\pi$ as well as water bridge linkages are used to stabilize the conformation of food dye. Moreover, comparative analyses ratified that the molecular structure, particularly the substituent species on the benzene ring of food dye, may exert a great impact on its toxicological properties. The biologically relevant model delineated here probably could be used for appraising the molecular toxicity of other food dyes, and in the long run, may offer valid information for food administration risk managers in relation to food additives.

AUTHOR INFORMATION

Corresponding Author

*E-mail: alexf.ting@gmail.com, feiding@cau.edu.cn (F.D.); pyk2009@nwsuaf.edu.cn (Y.-K.P.). Fax/Tel.: +86-29-87092367.

Author Contributions

●These authors contributed equally to this work.

Funding

This work was funded by grant support from the National Natural Science Foundation of China (No. 21272265).

Notes

The authors declare no competing financial interest.

■ ACKNOWLEDGMENTS

We are particularly indebted to Professor Ulrich Kragh-Hansen of Department of Medical Biochemistry, University of Aarhus, for the valuable gift of his doctoral dissertation. We offer heartfelt appreciation to Dr. Elizabeth J. Waters of Grape and Wine Research and Development Corporation, Australian Government, for her gentle support during the manuscript processing. Thanks also go to the reviewers of this article for their invaluable and constructive suggestions.

■ ABBREVIATIONS USED

ADD, attention deficit disorder; ADHD, attention deficit hyperactivity disorder; ADMET, absorption, distribution, metabolism, excretion and toxicity; Ala, alanine; ANOVA, analysis of variance; ANS, 8-anilino-1-naphthalenesulfonic acid; Asn, asparagine; CD, circular dichroism; DNA, DNA; FRET, Förster resonance energy transfer; IRF, instrument response function; R, correlation coefficient; ROS, reactive oxygen species; SD, standard deviation; Tris, tris(hydroxymethyl)-aminomethane; Trp, tryptophan

■ REFERENCES

(1) Ferreira, G. R.; Garcia, H. C.; Couri, M. R. C.; Santos, H. F. D.; de Oliveira, L. F. C. On the azo/hydrazo equilibrium in Sudan I azo dye derivatives. *J. Phys. Chem. A* **2013**, *117*, 642−649.

(2) Almeida, M. R.; Stephani, R.; Santos, H. F. D.; de Oliveira, L. F. C. Spectroscopic and theoretical study of the "azo"-dye E124 in condensate phase: Evidence of a dominant hydrazo form. *J. Phys. Chem A* **2010**, *114*, 526−534.

(3) Hsu, C.-A.; Wen, T.-N.; Su, Y.-C.; Jiang, Z.-B.; Chen, C.-W.; Shyur, L.-F. Biological degradation of anthroquinone and azo dyes by a novel laccase from *Lentinus* sp. *Environ. Sci. Technol.* **2012**, *46*, 5109−5117.

(4) Kobylewski, S.; Jacobson, M. F. Toxicology of food dyes. *Int. J. Occup. Environ. Health.* **2012**, *18*, 220−246.

(5) Cheung, W.; Shadi, I. T.; Xu, Y.; Goodacre, R. Quantitative analysis of the banned food dye Sudan-1 using surface enhanced Raman scattering with multivariate chemometrics. *J. Phys. Chem. C* **2010**, *114*, 7285−7290.

(6) Seiber, J. N.; Kleinschmidt, L. From detrimental to beneficial constituents in foods: Tracking the publication trends in JAFC. *J. Agric. Food Chem.* **2012**, *60*, 6644−6647.

(7) Radomski, J. L. Toxicology of food colors. *Annu. Rev. Pharmacol.* **1974**, *14*, 127−137.

(8) Swanson, J. M.; Kinsbourne, M. Food dyes impair performance of hyperactive children on a laboratory learning test. *Science* **1980**, *207*, 1485−1487.

(9) Bateman, B.; Warner, J. O.; Hutchinson, E.; Dean, T.; Rowlandson, P.; Gant, C.; Grundy, J.; Fitzgerald, C.; Stevenson, J. The effects of a double blind, placebo controlled, artificial food colourings and benzoate preservative challenge on hyperactivity in a general population sample of preschool children. *Arch. Dis. Child.* **2004**, *89*, 506−511.

(10) McCann, D.; Barrett, A.; Cooper, A.; Crumpler, D.; Dalen, L.; Grimshaw, K.; Kitchin, E.; Lok, K.; Porteous, L.; Prince, E.; Sonuga-Barke, E.; Warner, J. O.; Stevenson, J. Food additives and hyperactive behaviour in 3-year-old and 8/9-year-old children in the community: a randomised, double-blinded, placebo-controlled trial. *Lancet* **2007**, *370*, 1560−1567.

(11) Brown, M. A.; DeVito, S. C. Predicting azo dye toxicity. *Crit. Rev. Environ. Sci. Technol.* **1993**, *23*, 249−324.

(12) Hashem, M. M.; Atta, A. H.; Arbid, M. S.; Nada, S. A.; Asaad, G. F. Immunological studies on Amaranth, Sunset Yellow and Curcumin as food colouring agents in albino rats. *Food Chem. Toxicol.* **2010**, *48*, 1581−1586.

(13) Brown, J. P.; Roehm, G. W.; Brown, R. J. Mutagenicity testing of certified food colors and related azo, xanthene and triphenylmethane dyes with the Salmonella/microsome system. *Mutat. Res., Fundam. Mol. Mech. Mutagen.* **1978**, *56*, 249−271.

(14) Chung, K.-T.; Fulk, G. E.; Andrews, A. W. Mutagenicity testing of some commonly used dyes. *Appl. Environ. Microbiol.* **1981**, *42*, 641−648.

(15) Chung, K.-T. The significance of azo-reduction in the mutagenesis and carcinogenesis of azo dyes. *Mutat. Res., Rev. Genet. Toxicol.* **1983**, *114*, 269−281.

(16) Malachová, K.; Pavlícková, Z.; Novotný, C.; Svobodová, K.; Lednická, D.; Musílková, E. Reduction in the mutagenicity of synthetic dyes by successive treatment with activated sludge and the ligninolytic fungus, *Irpex lacteus*. *Environ. Mol. Mutagen.* **2006**, *47*, 533−540.

(17) Sharma, S.; Sharma, S.; Upreti, N.; Sharma, K. P. Monitoring toxicity of an azo dye methyl red and a heavy metal Cu, using plant and animal bioassays. *Toxicol. Environ. Chem.* **2009**, *91*, 109−120.

(18) Bonser, G. M.; Bradshaw, L.; Clayson, D. B.; Jull, J. W. A further study of the carcinogenic properties of ortho hydroxy-amines and related compounds by bladder implantation in the mouse. *Br. J. Cancer* **1956**, *10*, 539−546.

(19) Chung, K.-T.; Stevens, S. E., Jr. The reduction of azo dyes by the intestinal microflora. *Crit. Rev. Microbiol.* **1992**, *18*, 175−190.

(20) Tsuda, S.; Murakami, M.; Matsusaka, N.; Kano, K.; Taniguchi, K.; Sasaki, Y. F. DNA damage induced by red food dyes orally administered to pregnant and male mice. *Toxicol. Sci.* **2001**, *61*, 92−99.

(21) Combes, R. D.; Haveland-Smith, R. B. A review of the genotoxicity of food, drug and cosmetic colours and other azo, triphenylmethane and xanthenes dyes. *Mutat. Res., Rev. Genet. Toxicol.* **1982**, *98*, 101−243.

(22) Yadav, A.; Kumar, A.; Dwivedi, P. D.; Tripathi, A.; Das, M. In vitro studies on immunotoxic potential of Orange II in splenocytes. *Toxicol. Lett.* **2012**, *208*, 239−245.

(23) Nuin, E.; Andreu, I.; Torres, M. J.; Jiménez, M. C.; Miranda, M. A. Enhanced photosafety of cinacalcet upon complexation with serum albumin. *J. Phys. Chem. B* **2011**, *115*, 1158−1164.

(24) Bolel, P.; Mahapatra, N.; Halder, M. Optical spectroscopic exploration of binding of Cochineal Red A with two homologous serum albumins. *J. Agric. Food Chem.* **2012**, *60*, 3727−3734.

(25) Son, I.; Shek, Y. L.; Dubins, D. N.; Chalikian, T. V. Volumetric characterization of tri-*N*-acetylglucosamine binding to lysozyme. *Biochemistry* **2012**, *51*, 5784−5790.

(26) Fleming, A. On a remarkable bacteriolytic element found in tissues and secretions. *Proc. R. Soc. Lond. B: Biol. Sci.* **1922**, *93*, 306−317.

(27) Kirby, A. J. The lysozyme mechanism sorted—after 50 years. *Nat. Struct. Biol.* **2001**, *8*, 737−739.

(28) Haas, M.; Kluppel, A. C. A.; Wartna, E. S.; Moolenaar, F.; Meijer, D. K. F.; de Jong, P. E.; de Zeeuw, D. Drug-targeting to the kidney: renal delivery and degradation of a naproxen-lysozyme conjugate in vivo. *Kidney Int.* **1997**, *52*, 1693−1699.

(29) Phillips, R. A. Kidney. *Annu. Rev. Physiol.* **1949**, *11*, 493−526.

(30) Rennick, B. R. Renal excretion of drugs: tubular transport and metabolism. *Annu. Rev. Pharmacol.* **1972**, *12*, 141−156.

(31) Morrissey, K. M.; Stocker, S. L.; Wittwer, M. B.; Xu, L.; Giacomini, K. M. Renal transporters in drug development. *Annu. Rev. Pharmacol. Toxicol.* **2013**, *53*, 503−529.

(32) Lowry, O. H.; Rosebrough, N. J.; Farr, A. L.; Randall, R. J. Protein measurement with the Folin phenol reagent. *J. Biol. Chem.* **1951**, *193*, 265−275.

(33) Greenfield, N. J. Using circular dichroism spectra to estimate protein secondary structure. *Nat. Protoc.* **2006**, *1*, 2876−2890.

(34) Lakowicz, J. R. *Principles of Fluorescence Spectroscopy*, 3rd ed.; Springer Science + Business Media: New York, NY, 2006; pp 97−330.

(35) Bi, S. Y.; Ding, L.; Tian, Y.; Song, D. Q.; Zhou, X.; Liu, X.; Zhang, H. Q. Investigation of the interaction between flavonoids and human serum albumin. *J. Mol. Struct.* **2004**, *703*, 37−45.

(36) Monti, S.; Manet, I.; Marconi, G. Combination of spectroscopic and computational methods to get an understanding of supramolecular

chemistry of drugs: from simple host systems to biomolecules. *Phys. Chem. Chem. Phys.* **2011**, *13*, 20893−20905.
(37) Greenfield, N. J. Using circular dichroism collected as a function of temperature to determine the thermodynamics of protein unfolding and binding interactions. *Nat. Protoc.* **2006**, *1*, 2527−2535.
(38) Lloyd, J. B. F. Synchronized excitation of fluorescence emission spectra. *Nat. Phys. Sci.* **1971**, *231*, 64−65.
(39) Fuller, C. W.; Miller, J. N. Silver Medal lectures. *Proc. Anal. Div. Chem. Soc.* **1979**, *16*, 199−208.
(40) Abou-Zied, O. K. Spectroscopy of hydroxyphenyl benzazoles in solution and human serum albumin: detecting flexibility, specificity and high affinity of the warfarin drug binding site. *RSC Adv.* **2013**, *3*, 8747−8755.
(41) Lehrer, S. S. Solute perturbation of protein fluorescence. The quenching of the tryptophyl fluorescence of model compounds and of lysozyme by iodide ion. *Biochemistry* **1971**, *10*, 3254−3263.
(42) Paul, B. K.; Guchhait, N. A spectral deciphering of the binding interaction of an intramolecular charge transfer fluorescence probe with a cationic protein: thermodynamic analysis of the binding phenomenon combined with blind docking study. *Photochem. Photobiol. Sci.* **2011**, *10*, 980−991.
(43) De-Llanos, R.; Sánchez-Cortes, S.; Domingo, C.; García-Ramos, J. V.; Sevilla, P. Surface plasmon effects on the binding of antitumoral drug emodin to bovine serum albumin. *J. Phys. Chem. C* **2011**, *115*, 12419−12429.
(44) Mitra, P.; Banerjee, M.; Biswas, S.; Basu, S. Protein interactions of Merocyanine 540: spectroscopic and crystallographic studies with lysozyme as a model protein. *J. Photochem. Photobiol. B: Biol.* **2013**, *121*, 46−56.
(45) Chodera, J. D.; Mobley, D. L. Entropy-enthalpy compensation: role and ramifications in biomolecular ligand recognition and design. *Annu. Rev. Biophys.* **2013**, *42*, 121−142.
(46) Ross, P. D.; Subramanian, S. Thermodynamics of protein association reactions: forces contributing to stability. *Biochemistry* **1981**, *20*, 3096−3102.
(47) Abou-Zied, O. K.; Al-Lawatia, N.; Elstner, M.; Steinbrecher, T. B. Binding of hydroxyquinoline probes to human serum albumin: combining molecular modeling and Förster's resonance energy transfer spectroscopy to understand flexible ligand binding. *J. Phys. Chem. B* **2013**, *117*, 1062−1074.
(48) Kragh-Hansen, U. Structure and ligand binding properties of human serum albumin. *Dan. Med. Bull* **1990**, *37*, 57−84.
(49) Froehlich, E.; Mandeville, J. S.; Jennings, C. J.; Sedaghat-Herati, R.; Tajmir-Riahi, H. A. Dendrimers bind human serum albumin. *J. Phys. Chem. B* **2009**, *113*, 6986−6993.
(50) Imoto, T.; Forster, L. S.; Rupley, J. A.; Tanaka, F. Fluorescence of lysozyme: emissions from tryptophan residues 62 and 108 and energy migration. *Proc. Natl. Acad. Sci. U.S.A.* **1971**, *69*, 1151−1155.
(51) Stryer, L. Fluorescence spectroscopy of proteins. *Science* **1968**, *162*, 526−533.
(52) Stryer, L. The interaction of a naphthalene dye with apomyoglobin and apohemoglobin: a fluorescent probe of non-polar binding sites. *J. Mol. Biol.* **1965**, *13*, 482−495.
(53) Blake, C. C. F.; Koenig, D. F.; Mair, G. A.; North, A. C. T.; Phillips, D. C.; Sarma, V. R. Structure of hen egg-white lysozyme: a three-dimensional Fourier synthesis at 2 Å resolution. *Nature* **1965**, *206*, 757−761.
(54) Beechem, J. M.; Brand, L. Time-resolved fluorescence of proteins. *Annu. Rev. Biochem.* **1985**, *54*, 43−71.
(55) Stryer, L. Fluorescence energy transfer as a spectroscopic ruler. *Annu. Rev. Biochem.* **1978**, *47*, 819−846.
(56) Miller, J. N. Fluorescence energy transfer methods in bioanalysis. *Analyst* **2005**, *130*, 265−270.
(57) Clegg, R. M. The vital contributions of Perrin and Förster. *Biophoton. Int.* **2004**, *11*, 42−45.
(58) Bonan, S.; Fedrizzi, G.; Menotta, S.; Elisabetta, C. Simultaneous determination of synthetic dyes in foodstuffs and beverages by high-performance liquid chromatography coupled with diode-array detector. *Dyes Pigm.* **2013**, *99*, 36−40.
(59) Seiber, J. N.; Kleinschmidt, L. A. Contributions of pesticide residue chemistry to improving food and environmental safety: Past and present accomplishments and future challenges. *J. Agric. Food Chem.* **2011**, *59*, 7536−7543.
(60) Armbrust, K.; Burns, M.; Crossan, A. N.; Fischhoff, D. A.; Hammond, L. E.; Johnston, J. J.; Kennedy, I.; Rose, M. T.; Seiber, J. N.; Solomon, K. Perspectives on communicating risks of chemicals. *J. Agric. Food Chem.* **2013**, *61*, 4676−4691.
(61) Yadav, A.; Kumar, A.; Tripathi, A.; Das, M. Sunset yellow FCF, a permitted food dye, alters functional responses of splenocytes at non-cytotoxic dose. *Toxicol. Lett.* **2013**, *217*, 197−204.
(62) Iranfar, H.; Rajabi, O.; Salari, R.; Chamani, J. Probing the interaction of human serum albumin with ciprofloxacin in the presence of silver nanoparticles of three sizes: Multispectroscopic and ζ potential investigation. *J. Phys. Chem. B* **2012**, *116*, 1951−1964.
(63) Mansouri, M.; Pirouzi, M.; Saberi, M. R.; Ghaderabad, M.; Chamani, J. Investigation on the interaction between cyclophosphamide and lysozyme in the presence of three different kind of cyclodextrins: Determination of the binding mechanism by spectroscopic and molecular modeling techniques. *Molecules* **2013**, *18*, 789−813.
(64) Teilum, K.; Olsen, J. G.; Kragelund, B. B. Protein stability, flexibility and function. *Biochim. Biophys. Acta, Proteins Proteomics* **2011**, *1814*, 969−976.
(65) Sattar, Z.; Iranfar, H.; Asoodeh, A.; Saberi, M. R.; Mazhari, M.; Chamani, J. Interaction between holo transferrin and HSA-PPIX complex in the presence of lomefloxacin: An evaluation of PPIX aggregation in protein-protein interactions. *Spectrochim. Acta, Part A* **2012**, *97*, 1089−1100.
(66) Bourassa, P.; Bariyanga, J.; Tajmir-Riahi, H. A. Binding sites of resveratrol, genistein, and curcumin with milk α- and β-caseins. *J. Phys. Chem. B* **2013**, *117*, 1287−1295.
(67) Kanakis, C. D.; Tarantilis, P. A.; Polissiou, M. G.; Tajmir-Riahi, H. A. Probing the binding sites of resveratrol, genistein, and curcumin with milk β-lactoglobulin. *J. Biomol. Struct. Dyn.* **2012**, *12*, 1455−1466.
(68) Tsuda, S.; Matsusaka, N.; Madarame, H.; Ueno, S.; Susa, N.; Ishida, K.; Kawamura, N.; Sekihashi, K.; Sasaki, Y. F. The comet assay in eight mouse organs: results with 24 azo compounds. *Mutat. Res., Genet. Toxicol. Environ. Mutagen.* **2000**, *465*, 11−26.
(69) Amin, K. A.; Hameid, H. A., II; Elsttar, A. H. A. Effect of food azo dyes tartrazine and carmoisine on biochemical parameters related to renal, hepatic function and oxidative stress biomarkers in young male rats. *Food Chem. Toxicol.* **2010**, *48*, 2994−2999.
(70) Tarantal, A. F.; Chen, H.; Shi, T. T.; Lu, C.-H.; Fang, A. B.; Buckley, S.; Kolb, M.; Gauldie, J.; Warburton, D.; Shi, W. Overexpression of transforming growth factor-β1 in fetal monkey lung results in prenatal pulmonary fibrosis. *Eur. Respir. J.* **2010**, *36*, 907−914.
(71) Mayi, T. H.; Daoudi, M.; Derudas, B.; Gross, B.; Bories, G.; Wouters, K.; Brozek, J.; Caiazzo, R.; Raverdi, V.; Pigeyre, M.; Allavena, P.; Mantovani, A.; Pattou, F.; Staels, B.; Chinetti-Gbaguidi, G. Human adipose tissue macrophages display activation of cancer-related pathways. *J. Biol. Chem.* **2012**, *287*, 21904−21913.
(72) Levy, Y.; Onuchic, J. N. Water mediation in protein folding and molecular recognition. *Annu. Rev. Biophys. Biomol. Struct.* **2006**, *35*, 389−415.
(73) Shaban, Z.; El-Shazly, S.; Ishizuka, M.; Kimura, K.; Kazusaka, A.; Fujita, S. PPARα-dependent modulation of hepatic CYP1A by clofibric acid in rats. *Arch. Toxicol.* **2004**, *78*, 496−507.
(74) Stiborová, M.; Martínek, V.; Schmeiser, H. H.; Frei, E. Modulation of CYP1A1-mediated oxidation of carcinogenic azo dye Sudan I and its binding to DNA by cytochrome b5. *Neuroendocrinol. Lett.* **2006**, *27*, 35−39.
(75) Stiborová, M.; Dračínská, H.; Martínek, V.; Svášková, D.; Hodek, P.; Milichovský, J.; Hejduková, Ž.; Brotánek, J.; Schmeiser, H. H.; Frei, E. Induced expression of cytochrome P450 1A and NAD(P)H:quinone oxidoreductase determined at mRNA, protein, and enzyme activity levels in rats exposed to the carcinogenic azo dye

1-phenylazo-2-naphthol (Sudan I). *Chem. Res. Toxicol.* **2013**, *26*, 290−299.
(76) Zhang, Y. Z.; Görner, H. Photoprocesses of chlorine e6 bound to lysozyme or bovin serum albumin. *Dyes Pigm.* **2009**, *83*, 174−179.
(77) Zhang, Y. Z.; Görner, H. Photoprocesses of xanthene dyes bound to lysozyme or serum albumin. *Photochem. Photobiol.* **2009**, *85*, 677−685.
(78) Morgan, D. L.; Dunnick, J. K.; Goehl, T.; Jokinen, M. P.; Matthews, H. B.; Zeiger, E.; Mennear, J. H. Summary of the National Toxicology Program benzidine dye initiative. *Environ. Health Perspect.* **1994**, *102*, 63−78.
(79) Feng, J. H.; Cerniglia, C. E.; Chen, H. Z. Toxicological significance of azo dye metabolism by human intestinal microbiota. *Front. Biosci., Elite Ed.* **2012**, *4*, 568−586.
(80) Stingley, R. L.; Zou, W.; Heinze, T. M.; Chen, H. Z.; Cerniglia, C. E. Metabolism of azo dyes by human skin microbiota. *J. Med. Microbiol.* **2010**, *59*, 108−114.